ORIGINAL ARTICLE

Frame element including effects of reinforcement slippage for nonlinear analysis of R/C structures

Suchart Limkatanyu[1] and Agarat Samakrattakit[2]

Abstract

Limkatanyu, S. and Samakrattakit, A.
Frame element including effects of reinforcement slippage for nonlinear analysis of R/C structures
Songklanakarin J. Sci. Technol., 2003, 25(2) : 213-226

This paper presents the formulation and application of the flexibility-based, reinforced concrete frame model with bond-slip. The formulation starts from the derivation of the governing differential equations (strong form) of the problem and then the flexibility-based, reinforced concrete frame model with bond-slip (weak form) is constructed to obtain the numerical solution of the problem. This numerical model is derived based on the principle of stationary complementary potential energy. Tonti's diagrams are employed to conveniently represent the governing equations for both strong and weak forms of the problem. This numerical model can be applied to both monotonic and cyclic loadings. The reinforced concrete column experimentally tested under cyclic loads is used to illustrate the model accuracy and to show the importance of bond-slip inclusion.

Key words : finite elements, bond-slip model, nonlinear analysis, flexibility-based formulation

[1]**Ph.D. (Structural Engineering),** [2]**M.Eng. (Structural Engineering), Department of Civil Engineering, Faculty of Engineering, Prince of Songkla University, Hat Yai, Songkhla 90112 Thailand.**
Corresponding e-mail : lsuchart@ratree.psu.ac.th
Received, 12 November 2002 Accepted, 22 January 2003

บทคัดย่อ

สุชาติ ลิ่มกตัญญู และ เอกรัฐ สมัครัฐกิจ

ชิ้นส่วนในโครงข้อแข็งคอนกรีตเสริมเหล็กที่รวมผลของการเลื่อนตัวของเหล็กเสริมสำหรับการวิเคราะห์แบบไม่เชิงเส้น

ว. สงขลานครินทร์ วทท. 2546 25(2) : 213-226

บทความนี้นำเสนอการจัดรูปแบบและการประยุกต์ของแบบจำลองโครงสร้างคอนกรีตเสริมเหล็ก (คสล.) บนพื้นฐานของเฟลกซิบิลิตี ที่พิจารณาผลของการเลื่อนตัวของเหล็กเสริม การจัดรูปแบบเริ่มต้นด้วยการศึกษาสมการอนุพันธ์ในรูปแบบพื้นฐาน (Strong Form) แล้วสร้างแบบจำลองโครงสร้าง คสล. ที่พิจารณาผลของการเลื่อนตัวของเหล็กเสริมในรูปแบบง่าย (Weak Form) เพื่ออธิบายผลเฉลยเชิงตัวเลข การสร้างแบบจำลองเชิงคณิตศาสตร์อาศัยหลักการของสเตชั่นเนอรี่ของพลังงานความเครียดประกอบ แผนภาพของ Tonti ถูกนำมาพิจารณาเพื่อแสดงสมการสามัญสำหรับรูปแบบพื้นฐาน และแบบง่าย แบบจำลองเชิงคณิตศาสตร์ในบทความนี้สามารถประยุกต์ได้ทั้งในกรณีแรงกระทำที่มีทิศทางเดียว และแรงแบบวัฏจักร การทดสอบเสา คสล.ภายใต้ แรงแบบวัฏจักรถูกใช้ตรวจสอบความถูกต้องของแบบจำลอง และแสดงความสำคัญของการคิดผลของการเลื่อนตัวของเหล็กเสริม

ภาควิชาวิศวกรรมโยธา คณะวิศวกรรมศาสตร์ มหาวิทยาลัยสงขลานครินทร์ อำเภอหาดใหญ่ จังหวัดสงขลา 90112

The accurate representation of the bond-slip effects is important in predicting the response of reinforced concrete (R/C) frames under both monotonic and cyclic loads. Under the assumption of full composite action between the concrete and the reinforcing bars, the stiffness and strength of R/C structures are overestimated, as is the energy dissipated during the loading cycles. A number of experimental tests on R/C subassemblages have shown the reduction in stiffness due to slip in the reinforcing bars above the foundations and in the beam-column connections. Bar pullout, which may be experienced in older structures with insufficient bar anchorages or bar splices, drastically reduces the strength of the R/C members. In order to realistically describe the behavior of R/C structures in static and dynamic nonlinear structural analysis, the inclusion of the bond-slip effects is essential.

In recent years, major advances in modeling the monotonic and cyclic response of R/C frame structures have been accomplished. Especially, frame models relying on the fiber-section models have found widespread uses in research and professional practices. Fiber models are used to compute the section interaction diagrams, beam deflections, nonlinear static and dynamic frame responses, etc. The main advantage of the fiber model is that it automatically couples the interaction between axial and bending effects. Existing fiber-section models, however, are normally based on the assumption that plane sections remain plane and that there is strain-compatibility between the concrete and the steel rebars, hence neglecting the bond-slip effects. This leads to an overprediction of the initial stiffness and of the hysteretic energy dissipation of the R/C members (Spacone *et al*., 1996). The simplest way to account for the bond-slip effects in frame elements is to add nonlinear rotational springs at the element ends (Rubiano-Benavides, 1998). Although simple, this way needs the formulation of an *ad-hoc* phenomenological moment-rotation law, and disrupts the continuity of the fibers between adjacent elements.

The R/C frame elements with bond-slip proposed in this work are different from those published to date in that different degrees of freedom are used for the concrete beam and for the bars with bond-slip. In other words, the bond-slip

between the steel bar and the surrounding concrete is computed directly as the difference in the steel and concrete displacements at the bar level. Aprile *et al*. (2001) have already successfully tested the general idea with the simple, stiffness-based formulation. The resulting model is computationally robust, but not very accurate. Therefore, a large number of elements are needed to gain sufficient accuracy, hence requiring high computational efforts. To date, several researchers (e.g. Zeris and Mahin, 1988) have investigated the use of assumed force fields for the development of nonlinear frame elements. This interest stems from two main observations: *a*) in some simplified cases the internal force distributions in frame elements are known "exactly". This is for exam-ple the case of the R/C beam element with perfect bond; *b*) in general, the force fields along the beam are smoother than the deformation fields, which may show large jumps in the inelastic regions, particularly where plastic hinges tend to form (i.e. in column bases, girder ends, beam-midspan, etc.). Consequently, the uses of force-shape functions in the flexibility-based formulation are an encouraging way to improve the accuracy of finite element models.

This paper presents the general theoretical framework of the flexibility-based formulation of R/C frame element with bond-slip in the steel bars. The beam section force-deformation relations are derived from the fiber section model. The derivation of the governing differential equations (strong form) of the R/C frame element with bond interfaces is presented first. The flexibility-based element formulation (weak forms) is presented next and establishes the core of this paper. The flexibility-based element is derived from the principle of stationary complementary potential energy functional. The Tonti's diagrams are used to concisely illustrate the governing equations of both the strong and the weak forms. The flexibility-based element is implemented in a finite element analysis program, FEAP (Taylor, 1998) and the experimental result of the laterally loaded R/C column is used to validate the element accuracy and to show the effects of reinforcement slippages.

Equations of R/C frame element with bond-slip (strong from)

Equilibrium

The free body diagram of an infinitesimal segment *dx* of R/C frame element with *n* bars with bond interfaces is shown in Figure 1. Only bond stresses tangential to the bars are considered in this formulation. The dowel effect in the bars is neglected. Based on the small-deformation assumption, all of the equilibrium conditions are considered in the undeformed configuration. Axial equilibriums in the beam component and in the bar *i* lead to the following equations:

$$\begin{aligned} &\frac{dN_B(x)}{dx} + \sum_{i=1}^{n} D_{bi}(x) = 0 \\ &\frac{dN_i(x)}{dx} - D_{bi}(x) = 0 \ , \ i = 1, \ n \end{aligned} \tag{1}$$

where $N_B(x)$ and $N_i(x)$ are the axial forces in the beam and in the bar *i*, respectively. $D_{bi}(x)$ is the bond interface force per unit length between the beam and bar *i*. Vertical equilibrium of the infinitesimal segment *dx* yields :

$$\frac{dV_B(x)}{dx} - p_y(x) = 0 \tag{2}$$

where $V_B(x)$ is the beam section shear force and $p_y(x)$ is the transverse distributed load. Finally, moment equilibrium yields:

$$\frac{dM_B(x)}{dx} - V_B(x) - \sum_{i=1}^{n} y_i D_{bi}(x) = 0 \tag{3}$$

where $M_B(x)$ is the beam section bending moment, y_i is the distance of bar *i* from the element reference axis (Figure 1). This work follows the Euler-Bernoulli beam theory, thus the shear deformations are neglected. The shear force $V_B(x)$ is removed by combining Eqs. (2) and (3) to obtain

$$\frac{d^2 M_B(x)}{dx^2} - p_y(x) - \sum_{i-1}^{n} y_i \frac{dD_{bi}(x)}{dx} = 0 \tag{4}$$

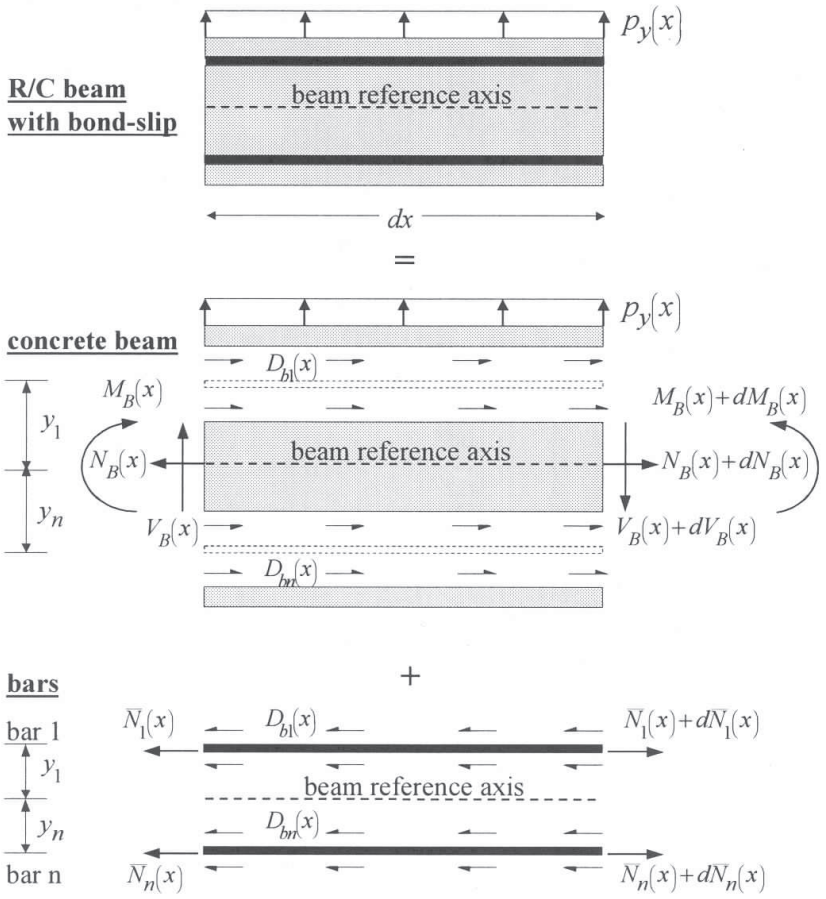

Figure 1. R/C beam element with bond-slip: Beam and bar components

Eqs. (1) and (4) represent the governing equilibrium equations of the R/C frame element with bond slip. Eqs. (1) and (4) can be written in the following matrix form:

$$\partial_B^T \mathrm{D}_B(x) - \partial_b^T \mathrm{D}_b(x) - \mathrm{p}(x) = 0 \qquad (5)$$

where $D_B(x)$ $\{\bar{\mathrm{D}}(x) \vdots \bar{\bar{\mathrm{D}}}(x)\}^T$ are the element section forces, $\bar{\mathrm{D}}(x) = \{N_B(x)\ M_B(x)\}^T$ are the beam section forces, $\bar{\bar{\mathrm{D}}}(x) = \{N_1(x) \cdots N_n(x)\}^T$ are the bar forces, $\mathrm{D}_b(x) = \{D_{b1}(x) \cdots D_{bn}(x)\}^T$ are the bond section forces and $\mathrm{p}(x) = \{0 \quad p_y(x) \quad 0 \cdots 0\}^T$ is the element force vector. ∂_B and ∂_b are differential operators defined in Appendix II. It is important to point out that there are $2n + 2$ internal force unknowns while only n+2 equilibrium equations are available at any element section. Consequently, this system is internally statically indeterminate and the internal forces cannot be determined solely by the equilibrium conditions.

Compatibility

The element section deformation vector conjugate of $\mathrm{D}_B(x)$ is $\mathrm{d}_B(x) = \{\bar{\mathrm{d}}(x) \vdots \bar{\bar{\mathrm{d}}}(x)\}^T$, where $\bar{\mathrm{d}}(x) = \{\varepsilon_B(x) \quad \kappa_B(x)\}^T$ are the beam section deformations (axial strain ε_B at reference axis and curvature κ_B) , and $\bar{\bar{\mathrm{d}}}(x) = \{\varepsilon_1(x) \cdots \varepsilon_n(x)\}^T$ contains the axial strains of the n bars. The following displacements are defined at the element level: $\mathrm{u}(x) = \{\bar{\mathrm{u}}(x) \vdots \bar{\bar{\mathrm{u}}}(x)\}^T$ are the displacement fields

along the element, where $\bar{u}(x) = \{u_B(x) \quad v_B(x)\}^T$ contains the beam axial and transverse displacements, respectively, and $\bar{\bar{u}}(x) = \{u_i(x) \cdots u_n(x)\}^T$ contains the axial dis-placements of the *n* bars.

From the small deformation assumption, the element deformations are related to the element displacements through the following compatibility relations: $\varepsilon_B(x) = du_B(x)/dx$, $\kappa_B(x) = d^2v_B(x)/dx^2$, and $\varepsilon_i(x) = du_i(x)/dx$, which can be written in the following matrix form:

$$\mathrm{d}_B(x) = \partial_B \mathrm{u}(x) \tag{6}$$

The bond slips are determined by the following compatibility relation between the beam and the bar displacements:

$$u_{bi}(x) = u_i(x) - u_B(x) + y_i \frac{dv_B(x)}{dx} \tag{7}$$

where $u_{bi}(x)$ is the bond slip between the beam and bar i. If the bond deformation vector $\mathrm{d}_b(x) = \{u_{b1}(x) \cdots u_{\mathrm{bn}}(x)\}^T$ is introduced, Eq. (7) can be written in the following matrix form:

$$d_b(x) = \partial_b \mathrm{u}(x) \tag{8}$$

Force-Deformation relations

The nonlinear nature of the proposed elements derives entirely from the nonlinear relation between the section forces $D_B(x)$, $D_b(x)$ and the section deformation $d_B(x)$, $d_b(x)$. In the proposed formulations, the fiber section model shown in Figure 2 is used to derive the constitutive law $D_B = D_B(d_B)$. The fiber model automatically accounts for the coupling between axial and bending responses. The Kent and Park (1971) law is used for the concrete fibers. The Menegotto and Pinto (1973) law is used for the bars. The explicit expression for the fiber beam section force deformation is given in Spacone *et al*. (1996). For the bond-slip constitutive relations $D_b = D_b(d_b)$, the Eligehausen *et al*. (1983) law is used. All of these uniaxial laws are shown in Figure 2.

In the following formulations, the section and bond-slip nonlinear laws are linearized ac-

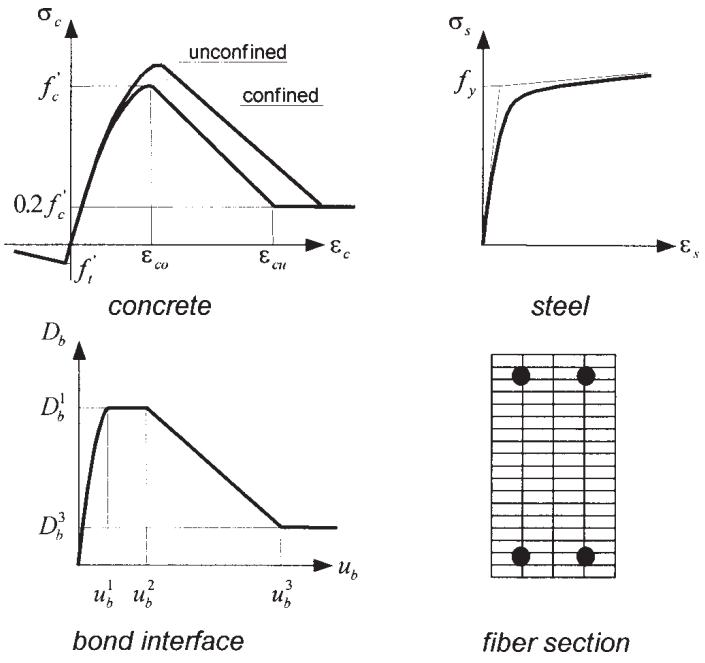

Figure 2. R/C beam element: Section fiber discretization and material uniaxial laws

cording to the following forms:

$$\begin{aligned} D_B(x) &= \mathrm{D}_B^0(x) + \Delta \mathrm{D}_B(x) = \mathrm{D}_B^0(x) + \mathrm{k}_B^0(x)\Delta \mathrm{d}_B(x) \\ D_b(x) &= \mathrm{D}_b^0(x) + \Delta \mathrm{D}_b(x) = \mathrm{D}_b^0(x) + \mathrm{k}_b^0(x)\Delta \mathrm{d}_b(x) \end{aligned} \tag{9}$$

where $\mathrm{D}_B^0(x)$, $\mathrm{D}_b^0(x)$, $\mathrm{k}_B^0(x)$ and $\mathrm{k}_b^0(x)$ are the section and bond force vectors and stiffness matrices at the initial point. The consistent inverse of (9) can be expressed in the following forms:

$$\begin{aligned} d_B(x) &= \mathrm{d}_B^0(x) + \Delta \mathrm{d}_B(x) = \mathrm{d}_B^0(x) + \mathrm{f}_B^0(x)\Delta \mathrm{D}_B(x) \\ d_b(x) &= \mathrm{d}_b^0(x) + \Delta \mathrm{d}_b(x) = \mathrm{d}_b^0(x) + \mathrm{f}_b^0(x)\Delta \mathrm{D}_b(x) \end{aligned} \tag{10}$$

where $\mathrm{d}_B^0(x)$, $\mathrm{d}_b^0(x)$, $\mathrm{f}_B^0(x)$ and $\mathrm{f}_b^0(x)$ are the section and bond deformation vectors and flexibility matrices at the initial point. In the above equations and throughout the paper, superscript 0 indicates the value of a vector or matrix at the initial point of the nonlinear scheme.

The compatibility, equilibrium and constitutive equations for the R/C frame element with bond-slip presented above are conveniently represented in the classical Tonti's diagram of Figure 3. This diagram is going to be modified for the different element formulations. Finally, for simplicity, the transverse load $p_y(x)$ is omitted in the following derivations.

Flexibility-based (force-hybrid) formulation (weak form)

The flexibility-based formulation stems from the flexibility-based steel-concrete composite beam element with partial interaction proposed by Salari *et al*. (1998). The flexibility-based formulation is derived from the total complementary potential energy functional and is the dual of the stiffness-based formulation. The element internal force fields $\mathrm{D}_B(x)$ and $\mathrm{D}_b(x)$ serve as the primary unknowns and are expressed in terms of the element nodal forces through appropriate force shape functions. The force shape functions are derived such that the equilibrium equations (5) are satisfied point-wise along the element. On the other hand, the beam compatibility equation (6) and the bond compatibility equation (8) are satisfied only in an integral sense. The steps involved in the flexibility-based formulation are schematically represented in the Tonti's diagram of Figure 4.

The total complementary potential energy functional Π_{CPE} is :

$$\begin{aligned} &\Pi_{CPE}[\mathrm{D}_B(x),\ \mathrm{D}_b(x)] = \\ &\int_L \mathrm{D}_B^T(x)(\mathrm{d}_B(x) - \partial_B \mathrm{u}(x))dx + \\ &\int_L \mathrm{D}_b^T(x)(\mathrm{d}_b(x) - \partial_b \mathrm{u}(x))dx \end{aligned} \tag{11}$$

According to the principle of stationary complementary potential energy, the compatible configuration is obtained when $_{CPE}$ reaches a

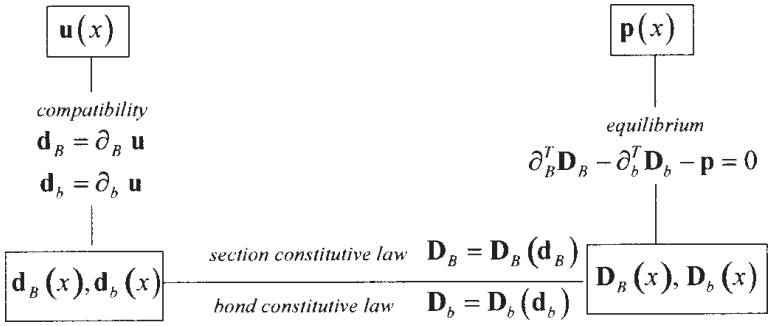

Figure 3. Tonti's diagram for R/C beam with bond-slip: Differential equations (strong form)

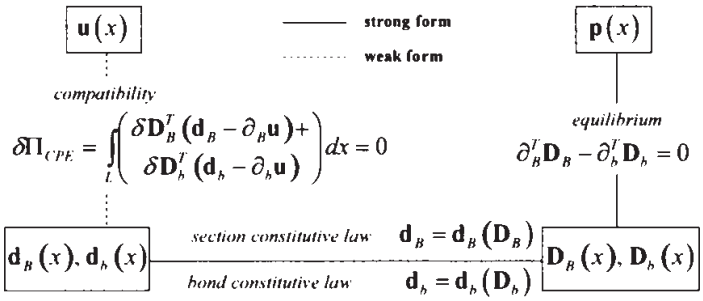

Figure 4. Tonti's diagram for R/C beam with bond-slip: Flexibility-based formulation

stationary value, i.e. when

$$\delta\Pi_{CPE}[\delta D_B(x),\ \delta D_b(x)] = \int_L \delta D_B^T(x)(d_B(x) - \partial_B u(x))dx + \int_L \delta D_b^T(x)(d_b(x) - \partial_b u(x))dx = 0 \qquad (12)$$

Upon substitution of the section linearized laws (10) , (12) is written

$$\delta\Pi_{CPE}\int_L \delta D_B^T(x)(d_B^0(x) + f_B^0(x)\Delta D_B(x) - \partial_B u(x))dx + \int_L \delta D_b^T(x)(d_b^0(x) + f_b^0(x)\Delta D_b(x) - \partial_b u(x))dx = 0 \qquad (13)$$

where $\delta D_B(x)$ and $\delta D_b(x)$ are virtual, equilibrated section and bond-interface force fields, respectively, and $f_B^0(x)$ and $f_b^0(x)$ are the initial flexibi-lity matrices of the section and of the bond-interfaces, respectively. Integration by parts of (13) and substitution of the equilibrium equation (5) lead to the following matrix equation:

$$\int_L \begin{Bmatrix}\delta D_B(x)\\ \delta D_b(x)\end{Bmatrix}^T \begin{bmatrix} f_B^0(x) & 0\\ 0 & f_b^0(x)\end{bmatrix}\begin{Bmatrix}\Delta D_B(x)\\ \Delta D_b(x)\end{Bmatrix}dx = \delta\overline{Q}^T\overline{U} - \int_L \begin{Bmatrix}\delta D_B(x)\\ \delta D_b(x)\end{Bmatrix}^T \begin{Bmatrix} d_B^0(x)\\ d_b^0(x)\end{Bmatrix}dx \qquad (14)$$

where $\delta\overline{Q}^T\overline{U}$ is the boundary term and represents the external virtual work done by $\delta\overline{Q}$ (the virtual element nodal forces without rigid body modes) on $\overline{U}$ (the corresponding element nodal displacements without rigid body modes). The element is formulated without rigid body modes in view of its implementation in a general-purpose finite element code, which requires inversion of the element flexibility matrix (Spacone *et al*. 1996). Eq. (14) is the backbone equation of the flexibility-based finite element formulation. To obtain the discrete form of (14), the section forces $D_B(x)$ and the bond-interface forces $D_b(x)$ are expressed in terms of the element nodal forces without rigid body modes $\overline{Q}$ and of the bond-interface forces $\overline{Q}_b$ at selected reference points along the interface, according to the following matrix relation:

$$\begin{Bmatrix}D_B(x)\\ D_b(x)\end{Bmatrix} = \begin{bmatrix} N_{BB}^{F\text{-}B}(x) & N_{Bb}^{F\text{-}B}(x)\\ N_{bB}^{F\text{-}B}(x) & N_{bb}^{F\text{-}B}(x)\end{bmatrix}\begin{Bmatrix}\overline{Q}\\ \overline{Q}_b\end{Bmatrix} \qquad (15)$$

where the superscript *F-B* denotes the flexibility-based formulation, and $N_{BB}^{F\text{-}B}(x)$, $N_{Bb}^{F\text{-}B}(x)$, $N_{bB}^{F\text{-}B}(x)$, $N_{bb}^{F\text{-}B}(x)$ are the force shape functions. Substitution of (15) into (14) and from the arbitrariness of $\delta\overline{Q}$ and $\delta\overline{Q}_b$, the following matrix expression results:

$$\begin{bmatrix} \bar{F}^{0}_{BB} & \bar{F}^{0}_{Bb} \\ \bar{F}^{0\,T}_{Bb} & \bar{F}^{0}_{bb} \end{bmatrix} \begin{Bmatrix} \Delta\bar{Q} \\ \Delta\bar{Q}_b \end{Bmatrix} = \begin{Bmatrix} \bar{U} \\ 0 \end{Bmatrix} - \begin{Bmatrix} \bar{r}^{0} \\ \bar{r}^{0}_{b} \end{Bmatrix} \tag{16}$$

where $\bar{F}^{0}_{BB}$, $\bar{F}^{0}_{Bb}$, $\bar{F}^{0}_{bb}$ are the following flexibility terms:

$$\begin{aligned} \bar{F}^{0}_{BB} &= \int_L \left(N^{F\text{-}B\,T}_{BB}\; f^{0}_{B}\; N^{F\text{-}B}_{BB} + N^{F\text{-}B\,T}_{bB}\; f^{0}_{b}\; N^{F\text{-}B}_{bB} \right) dx \\ \bar{F}^{0}_{Bb} &= \int_L \left(N^{F\text{-}B\,T}_{BB}\; f^{0}_{B}\; N^{F\text{-}B}_{Bb} + N^{F\text{-}B\,T}_{bB}\; f^{0}_{b}\; N^{F\text{-}B}_{bb} \right) dx \\ \bar{F}^{0}_{bb} &= \int_L \left(N^{F\text{-}B\,T}_{Bb}\; f^{0}_{B}\; N^{F\text{-}B}_{Bb} + N^{F\text{-}B\,T}_{bb}\; f^{0}_{b}\; N^{F\text{-}B}_{bb} \right) dx \end{aligned} \tag{17}$$

$\bar{r}^{0}$ and $\bar{r}^{0}_{b}$ represent the displacements at the element and bond degrees of freedom, respectively, compatible with the internal deformations d^{0}_{B} and d^{0}_{b}:

$$\begin{aligned} \bar{r}^{0} &= \int_L \left(N^{F\text{-}B\,T}_{BB}\; d^{0}_{B} + N^{F\text{-}B\,T}_{bB}\; d^{0}_{b} \right) dx \\ \bar{r}^{0}_{b} &= \int_L \left(N^{F\text{-}B\,T}_{Bb}\; d^{0}_{B} + N^{F\text{-}B\,T}_{bb}\; d^{0}_{b} \right) dx \end{aligned} \tag{18}$$

In fact, $\bar{U}$ - $\bar{r}^{0}$ and - $\bar{r}^{0}_{b}$ represent the element nodal and bond displacement residuals, respectively, in the flexibility equation (16). The zero term on the right-hand side of (16) implies that the relative bond-slips at the selected reference points along the interfaces are equal to zero. This condition is similar to the known displacement conditions that are used to determine the redundant forces in statically indeterminate structures by the classical force method.

The redundant force unknowns $\Delta\bar{Q}_b$ are eliminated through static condensation in (16). The second equation in (16) yields $\Delta\bar{Q}_b = -(\bar{F}^{0}_{bb})^{-1}(\bar{F}^{0}_{bB}\Delta\bar{Q} + \bar{r}^{0}_{b})$, which substituted in the first equation yields

$$\bar{F}^{0}\Delta\bar{Q} = \bar{U} - \bar{U}^{0}_{B} - \bar{U}^{0}_{b} \tag{19}$$

where $\bar{F}$ is element flexibility matrix defined as:

$$\bar{F}^{0} = \bar{F}^{0}_{BB} - \bar{F}^{0}_{Bb}(\bar{F}^{0}_{bb})^{-1}\bar{F}^{0}_{bB} \tag{20}$$

and $\bar{U}^{0}_{B}$, $\bar{U}^{0}_{b}$ are the contributions of the beam component and of the bond-interfaces, respectively, to the element nodal displacements $\bar{U}^{0}$ without rigid body modes:

$$\begin{aligned} \bar{U}^{0}_{B} &= \int_L \left(N^{F\text{-}B\,T}_{BB} - \bar{F}^{0}_{Bb}(\bar{F}^{0}_{bb})^{-1}\; N^{F\text{-}B\,T}_{Bb} \right) d^{0}_{B}\, dx \\ \bar{U}^{0}_{b} &= \int_L \left(N^{F\text{-}B\,T}_{bB} - \bar{F}^{0}_{Bb}(\bar{F}^{0}_{bb})^{-1}\; N^{F\text{-}B\,T}_{bb} \right) d^{0}_{b} dx \end{aligned} \tag{21}$$

The right-hand side vector $\bar{U}$ - $\bar{U}^{0}_{B}$ - $\bar{U}^{0}_{b}$ of (19) represents the element nodal displacement residuals corresponding to the weak form of the compatibility conditions (6) , (8) and vanishes when the compatible configuration is reached.

Figure 5 shows the 2-node flexibility-based R/C frame element with and without rigid body modes. Adding the rigid body modes to the element of Figure 5b or filtering-out the rigid body modes from the element of Figure 5a is accomplished through matrix transformations based on equilibrium and compatibility between the two systems.

In structures that are internally statically determinate, such as the R/C beam with perfect bond of Spacone *et al*. (1996), the internal force distributions can be determined exactly from equilibrium. It is also important to remark that in this case only beam deformation contributes to the total complementary potential energy functional Π_{CPE}. In the R/C beam model with bond-slip of Figure 5, which is internally statically indeterminate, the internal force distributions cannot be exactly determined from equilibrium only, except for some special, simple linear-elastic structures. The bond-interface forces serve as the redundant forces in this element. Assumptions on the bond force distributions are made. This procedure is identical to that followed by Salari *et al*. (1998) for the steel-concrete composite beam with deformable shear connectors. In the proposed formulation of a R/C element with bond-slip, the bond-force distributions are assumed to be cubic functions. During the element development, a quadratic bond-interface force distribution was

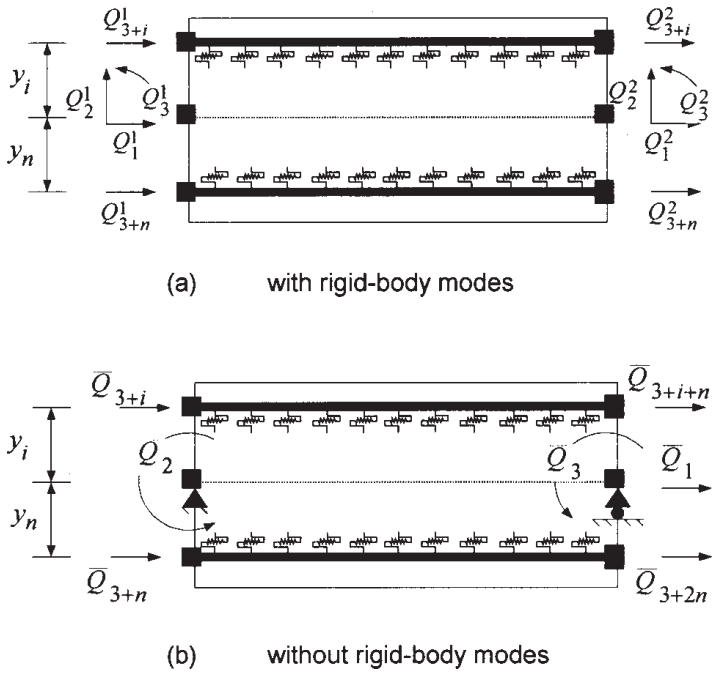

Figure 5. 2-Node flexibility-based R/C element with bond-slip

also tested, but it was discarded because it did not accurately represent the actual bond distribution. The beam axial force and bending moment and the bar axial force distributions corresponding to the cubic bond-interface force distributions are quartic functions.

Low-Moehle Specimen 1 (Low and Moehle, 1987)

A series of R/C cantilever columns with rectangular cross section were tested by Low and Moehle (1987). A constant axial force representing the gravity load and cyclic lateral displacements representing seismic actions were applied to the columns. One of these columns, referred as Low-Moehle Specimen 1, was modeled by Spacone *et al*. (1996) to validate the flexibility-based formulation of a R/C frame element with perfect bond. Though the correlation study between experimental and numerical results was rather satisfactory in aspects of strength, the experimental result was more flexible than the numerical solution. This is due to the fact that the model with perfect bond could not represent the base rotations resulting from the large slips of the reinforcing bars in the anchorage zone. The same specimen is used herein to verify the proposed model accuracy and to show the effects of reinforcement slippages.

Figure 6 shows the specimen geometry. The column was subjected to a constant axial compression of 44.5 kN (approximately 5% $f_c' A_g$) and a cyclic lateral displacement causing flexure about the weak axis. According to the report by Low and Moehle (1987) and using the labeling of Figure 6, the material properties are: f_y 447.5 MPa for rebar set I, f_y 444 MPa for rebar set II and f_y 504 MPa for rebar set III. The ultimate compressive strengths of unconfined and confined concrete are 36.54 MPa and 42.13 MPa, respectively. The tensile strength of concrete, though considered in the analyses, does not affect the results, except at the very early loading stages, before the base section cracks. As for the bond

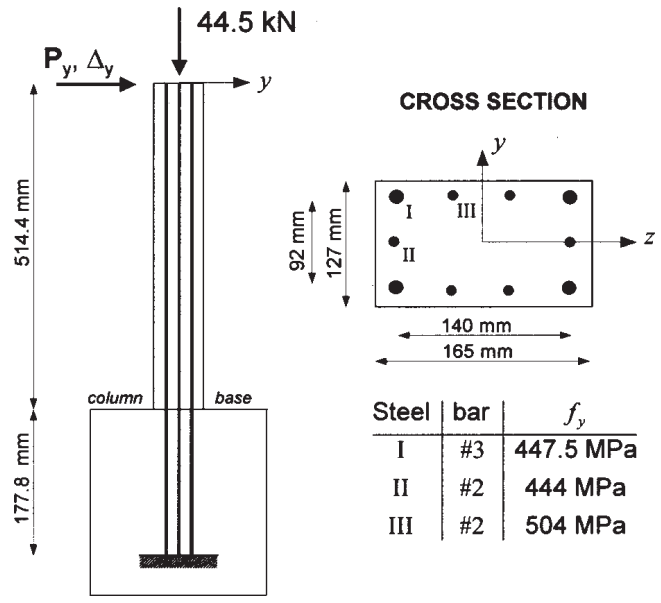

Figure 6. Geometry and loads of Low-Moehle Specimen 1

stress-slip relation, in the test bond did not fail or reach the plateau shown in Figure 2, thus only the ascending branch of the bond-slip envelope is of interest. The simple linear model is used with stiffness of 8.75 MPa/mm for bar set I (bars #3) and 9.05 MPa/mm for bar set II and III (bars #2). These values are based on a set of formulas developed by Monti *et al*. (1994) from the regression analysis on a number of pullout tests available in the published literature. In the numerical model, the column is discretized into 1 element, plus 1 element representing the anchorage zone. In the original test specimen, the rebars were hooked 7 in. (177.8 mm) into the foundation. To simulate the effect of the hooks, the bar nodes are assumed fully anchored 7 in. into the foundation (Figure 6).

Figure 7a compares the tip force-displacement response from the experimental test with the numerical result obtained with the flexibility-based R/C frame element with perfect bond (Spacone *et al*., 1996), while Figure 7b superimposes the tip force-displacement response from the experimental test with the numerical result obtained with the flexibility-based R/C frame element with bond-interfaces proposed in this study. As expected, both models predict the same column strength. Bond-slip mostly affects the column stiffness and the shape of the unloading-reloading curves. The model without bond-slip over-predicts the hysteretic energy of the specimen. During unloading, initial unloading is followed by closing of the crack, reloading and yielding of the steel in tension. With the model with bond-slip, when the column unloads, closing of the crack is accompanied by slip of the rebars at the column base. This gives a more flexible response, and yielding of the rebars in tension is delayed. It should be noted that the initial unloading stiffness predicted by the proposed model is somehow more flexible than the experimental one. This is mostly due to the selection of a linear unloading branch for the bond law. A more refined curve would yield a smoother trend, but the overall response of the model would be unaffected. The specimen initial stiffness is also smaller for the model with bond-slip, since some slip is present from the initial phases of loading, as shown in a number of tests on R/C columns and frames.

In order to show the effects of bond-slip

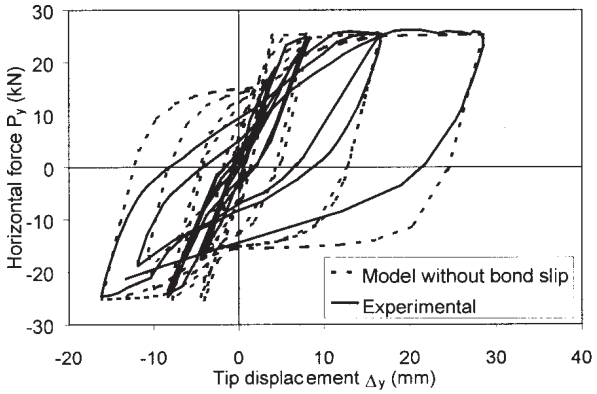

(a)

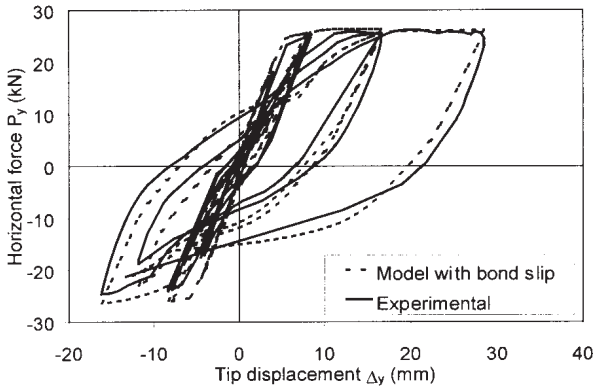

(b)

Figure 7. Experimental and analytical responses of Low-Moehle Specimen 1 (a) Model with perfect bond; (b) Model with bond-slip

on the section strains, Figure 8 shows the strain distribution at the column base corresponding to a positive tip displacement of approximately 17 mm. The loss of section planarity is apparent from the differences in the concrete and steel strains. In tension, the steel strains are considerably smaller than the corresponding concrete strains. In compression, the steel strains are still in tension, because the rebars have first yielded in tension, thus compression stresses can develop under tensile strains. The large steel strains observed in Figure 8 conform with the strain magnitudes reported

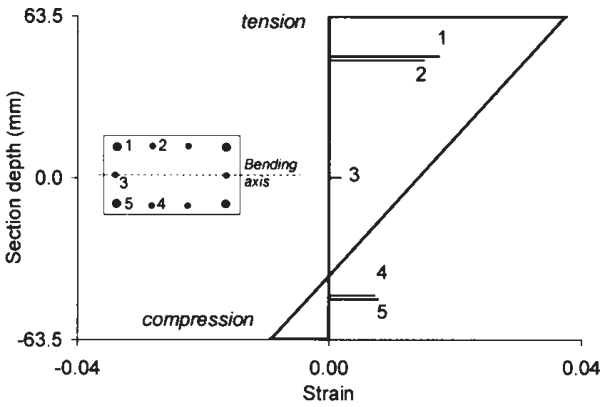

Figure 8. Strain distributions in concrete and steel at column base corresponding to a tip displacement of approximately 17 mm.

in Low and Moehle (1987).

Figure 9 compares the stress-strain relations of bar I obtained from the models with bond-slip and without bond-slip at the column-base section during the loading history. It is clear that in the model without bond-slip the amount of input energy is dissipated through larger full cycles of the stress-strain model of reinforcing bars, while in the model with bond-slip a lesser amount of the input energy is dissipated through the inelastic behavior of reinforcing bars with the remaining energy being dissipated in the slip between concrete and reinforcing bars. This explains why the model without bond-slip of Figure 7 overpredicts the hysteretic energy.

As previously noted, bond remained mostly elastic in the above test. The bond characteristics and the rebar anchorage prevented bond failure and bar pullout. In order to explore the proposed model characteristics, the rebar anchorage of the original column was modified. Anchorage lengths of 1 in. (25.4 mm), 3 in. (76.2 mm), 5 in. (127 mm) and 7 in. (177.8 mm) were considered. The bond strength was also reduced to 25% that of the original value. A monotonically increasing displacement was applied at the column tip. The effect of the different anchorage lengths is shown in Figure 10. Only the column with l_{an} = 7 in. reaches the

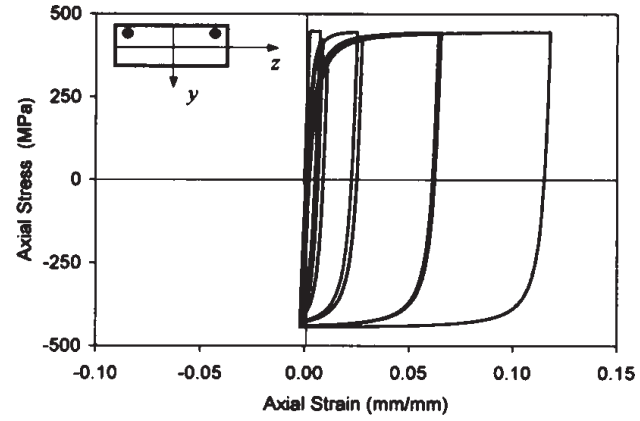

(a)

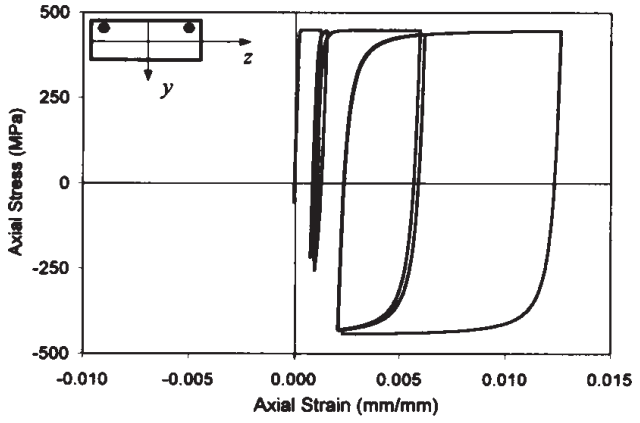

(b)

Figure 9. Stress-strain loading history of bar I: (a) Model without bond-slip; (b) Model with bond-slip

strength of the original column of Figure 7. In this case bond fails at the column base but the rebars in tension do not totally pull-out because the steel rebars yield before bond can fail throughout the anchorage length. On the other end, for shorter anchorage lengths the column fails because of complete bar pull-out from the foundation block, while the steel rebars remain linear elastic.

Summary and Conclusions

This paper presents the derivation of the governing differential equations (strong form) and derives the flexibility-based finite element formulation (weak forms) for the R/C frame element with bond-interfaces. The flexibility-based (force hybrid) element is derived from the principle of stationary total complementary potential energy functional and employs force-shape functions to express the internal force fields in terms of force degrees of freedom. In this element, the element bond forces at selected reference points serve as internal redundant forces, and are statically condensed out in order to implement the element into a general-propose stiffness-based finite element program. As a result, the bond force continuity

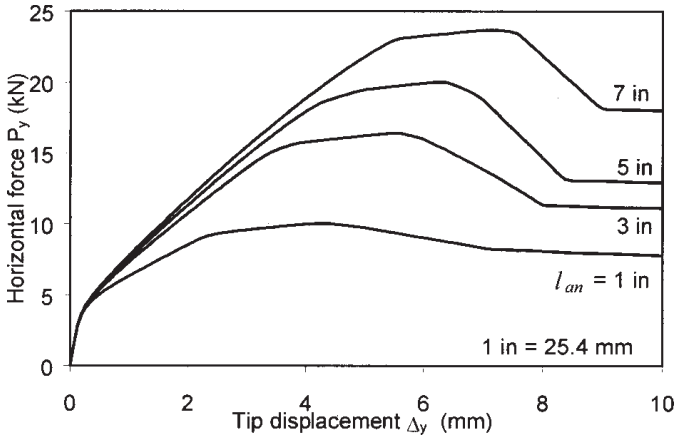

Figure 10. Column response with weak bond and reduced anchorage length

between adjacent elements is locally relaxed. Tonti's diagrams are also used to schematically represent the set of basic governing equations for both strong and weak forms.

The correlation study between experimental and numerical results of a R/C column subjected to cyclic loading is used to show the importance of bond-slip in modeling the response of R/C structures and to validate the model formulation. The inclusion of bond-slip effects results in a prediction of the experimental results that is much more accurate than that obtained with a fiber model without bond-slip. The model can also trace failure of the column by bar pull-out. Pull-out tests can be extended to different bar materials, such as mild steel, prestressing steel and FRP bars. Pull-out studies can be performed to study of the effects of bond and anchorage lengths for enhancing design provisions.

Notation

$$\partial_B = \begin{bmatrix} \frac{d}{dx} & 0 & \vdots & 0 & \mathbf{0} & 0 \\ 0 & \frac{d^2}{dx^2} & \vdots & 0 & \mathbf{0} & 0 \\ \cdots & \cdots & \cdots & \cdots & \cdots & \cdots \\ 0 & 0 & \vdots & \frac{d}{dx} & \cdots & 0 \\ \mathbf{0} & \mathbf{0} & \vdots & \mathbf{0} & \cdots & \mathbf{0} \\ 0 & 0 & \vdots & 0 & \cdots & \frac{d}{dx} \end{bmatrix} = \text{beam differential operator ;}$$

$$\partial_b = \begin{bmatrix} -1 & y_1 \frac{d}{dx} & 1 & \mathbf{0} & 0 \\ \cdots & \cdots & \cdots & \cdots & \cdots \\ -1 & y_n \frac{d}{dx} & 0 & \mathbf{0} & 1 \end{bmatrix} = \text{bond differential operator.}$$

References

Aprile, A., Spacone, E., and Limkatanyu, S. 2001. Role of bond in beams strengthened with steel and FRP plates, ASCE J. of Structural Engineering, 127(12) : 1445-1452.

Eligehausen, R., Popov, E.P., and Bertero, V.V. 1983. Local bond stress-slip relationships of deformed bars under generalized excitations: experimental results and analytical model. EERC Report 83-23, Earthquake Engineering Research Center, University of California, Berkeley.

Kent, D.C. and Park, R. 1971. Flexural members with confined Concrete. ASCE Journal of the Structural Division, 97(7) : 1964-1990.

Low, S.S., and Moehle, J.P. 1987. Experimental Study of Reinforced Concrete Columns Subjected to Multi-Axial Cyclic Loading. EERC Report 87/14, Earthquake Engineering Research Center, University of California, Berkeley.

Menegotto, M., and Pinto, P.E. 1973. Method of analysis for cyclically loaded reinforced concrete plane frames including changes in geometry and nonelastic behavior of elements under combined normal force and bending. IABSE Symposium on Resistance and Ultimate Deformability of Structures Acted on by Well-Defined Repeated Loads, Lisbon, Portugal: 112-123.

Monti, G., De Sortis, A., and Nuti, C. 1994. Problemi di scala nella sperimentazione pseudodinamica di pile da ponte in C.A. (in Italian). Proceedings, Workshop Danneggiamento, Prove Cicliche e Pseudodinamica, (Damage, Cyclic Tests and Pseudo-dynamic Testing), Napoli, Italy.

Rubiano-Benavides, N.R. 1998. Predictions of the inelastic seismic response of concrete structures including shear deformations and anchorage slip (Ph.D. dissertation), Department of Civil Engineering, University of Texas, Austin.

Salari, M.R., Spacone, E., Shing P.B, D.M. Frangopol. 1998. Nonlinear analysis of composite beams with deformable shear connectors, ASCE J. of Structural Engineering, 124(10) : 1148-1158.

Spacone, E., Filippou, F.C., and Taucer, F.F. 1996. Fibre beam-column model for nonlinear analysis of R/C frames. Part I: formulation, Earthquake Engineering and Structural Dynamics, 25: 711-725.

Taylor, R.L. 1998. FEAP: A Finite Element Analysis Program. User manual: Version 7.1, Department of Civil and Environmental Engineering, University of California, Berkeley.

Zeris, C.A. and Mahin, S.A. 1988. Analysis of reinforced concrete beam-columns under uniaxial excitation, ASCE J. of Structural Engineering, 114(4) : 804-820.